Cellular Signalling 54 (2019) 102–114

Contents lists available at ScienceDirect

Cellular Signalling

journal homepage: www.elsevier.com/locate/cellsig

Effects of long non-coding RNA LINC00667 on renal tubular epithelial cell proliferation, apoptosis and renal fibrosis *via* the miR-19b-3p/LINC00667/CTGF signaling pathway in chronic renal failure

Wen Chen, Zhong-Qi Zhou, Yue-Qin Ren, Lei Zhang, Li-Na Sun, Yu-Lin Man, Zhi-Kui Wang*

Department of Nephrology, Linyi People's Hospital, No. 27, Jiefang Road, Linyi 276003, China

ARTICLE INFO

Keywords:
Long non-coding RNA LINC00667
MiR-19b-3p
CTGF
Chronic renal failure
Renal fibrosis

ABSTRACT

The global prevalence of chronic renal failure (CRF) has significantly elevated with various reports indicating there to be a 10% worldwide rate. The functions of long non-coding RNAs (lncRNAs) and their deeper association with CRF at present remain poorly understood. Hence, the aim of the present study was to investigate the altered expressions of lncRNA LINC00667 in CRF and its associated effects on renal tubular epithelial cell proliferation, apoptosis and renal fibrosis through the microRNA-19b-3p (miR-19b-3p)/LINC00667/connective tissue growth factor (CTGF) signaling pathway. Initially, verification of the targeting relationship between LINC00667, CTGF and miR-19b-3p was performed, after which evidence was obtained indicating that miR-19b-3p could negatively regulate LINC00667 and CTGF. The expressions of CTGF in both the CRF and normal renal tissues were determined by immunohistochemistry means, with LINC00667 and CTGF determined to be highly expressed, while poor expression levels of miR-19b-3p were detected among the CRF tissues. The expressions of LINC00667, miR-19b-3p, fibrosis- and epithelial-mesenchymal transition (EMT)-related genes were also examined. The successfully established CRF rat models were treated with varying mimics, inhibitors, and siRNA. ELISA was applied to determine the renal function-related factors. Besides, the renal cell proliferation, migration and apoptosis were detected. In response to LINC00667 silencing, the renal tubular epithelial cells displayed increased proliferation and migration accompanied by reduced apoptosis based on upregulated miR-19b-3p, along with inhibited renal fibrosis and EMT detected. Taken together, the key findings of our study demonstrated that decreased lncRNA LINC00667 could promote renal tubular epithelial cell proliferation and ameliorate renal fibrosis in CRF *via* the miR-19b-3p/LINC00667/CTGF signaling pathway.

1. Introduction

Chronic renal failure (CRF) is often defined as a glomerular filtration rate (GFR) persistently below 15 mL/min per 1·73 m^2 and represents the end stage of chronic kidney disease in accordance with the KDIGO 2012 Clinical Practice Guideline for the Evaluation and Management of Chronic Kidney Disease [1]. CRF represents the most prevalent public health condition among the elderly population worldwide, with histopathologically features comprised of tubulointerstitial fibrosis and glomerulosclerosis as the main source of kidney damage [2,3]. Chronic kidney disease (CKD) refers to a common pathology of glomerulosclerosis and tubulointerstitial fibrosis which is well-known as a predictive indicator of progression to end-stage disease [4]. Renal tubulointerstitial fibrosis might originate from a loss of tubulointerstitial volume, which produces a disproportionate increase in the density of matrix and promotes the progression of renal disease [5]. Patients diagnosed as CKD are at high risk of cardiovascular events, progression to kidney failure which is in need of chronic dialysis, and furthermore death [6]. There is a growing acknowledgement that CRF regarding the complexity of the disease which often requires a multifactorial therapeutic approach in order to remedy the shortcomings of more conventional therapies such as dialysis [7]. At present, there is no cure for CRF. Thus, there exists an urgent need to identify novel treatment methods to prevent the progression of renal fibrosis associated with CRF.

Long non-coding RNAs (lncRNAs) have a length of > 200 nucleotides and are essential factors involved in the regulation of mRNA stability, splicing, and recruitment transcription factors, with low or no protein coding potential [8,9]. A large number of studies have highlighted a correlation between lncRNA disorders and a variety of human

* Corresponding author.
E-mail address: wangzkep@163.com (Z.-K. Wang).

https://doi.org/10.1016/j.cellsig.2018.10.016
Received 24 March 2018; Received in revised form 24 October 2018; Accepted 25 October 2018
Available online 26 October 2018
0898-6568/

diseases, including various kinds of cancer, as well as renal disease [10–13]. For example, lncRNA-RCCRT1 has been reported to be highly expressed in renal cell carcinoma and promotes cell migration and invasion [14]. MiRNAs are short (~22 nucleotides) noncoding RNA molecules that play a key role in predicting cancer-specific survival in cases of renal cell carcinoma [15,16]. In our study, GSE37171 chip revealed that LINC00667 was up-regulated in CRF tissues. MiR-19b-3p, which belongs to both the clusters of miR-17-92 and miR-106-363, has been speculated to function in several human malignancies and has been identified as an independent predictor of poor survival among patients with nasopharyngeal carcinoma [17]. Importantly, the miR-17-92 cluster represents an essential element in embryo development, immune system, kidney and heart development and tumorigenicity [18]. Previous reports have presented evidence suggesting that the overexpression of miR-19b-1 triggers epithelial–mesenchymal transition (EMT) and enhances the migration and invasion of lung cancer cells, while in contrast silencing miR-19b-1 has been observed to reverse EMT and reduce cell migration and invasion abilities [19]. The knockdown of miR-17-92 cluster resulted in renal hypodysplasia and a striking albuminuria [20]. After we retrieved in the mirdb (http://www.mirdb.org/), starbase (http://starbase.sysu.edu.cn/index.php) and mirtarbase (http://mirtarbase.mbc.nctu.edu.tw/php/search.php) websites, Serine/threonine-protein phosphatase 2A 56-kDa regulatory subunit epsilon isoform (PPP2R5E), mineralocorticoid receptor (NR3C2), homeodomain-interacting protein kinase (3HIPK3), connective tissue growth factor (CTGF) and bone morphogenetic protein receptor-II (BMPR2) were identified as the target genes of microRNA-19b-3p (Supplementary Fig. 1). But only CTGF was associated with CKD [21]. Therefore, after the exploration of genetic databases, and identification of target genes, CTGF was chosen as the study subject. CTGF is an important profibrotic factor in kidney diseases [22]. Blockade of endogenous CTGF has been suggested to ameliorate experimental renal damage and inhibit synthesis of extracellular matrix in cultured renal cells [23]. Moreover, miRNA-19 has been proved to regulate CTGF expression in age-related heart failure [24]. The central objective of the present study was to identify a therapeutic target for the treatment of CRF. Hence, we asserted the hypothesis that lncRNA LINC00667 could regulate CRF fibrosis through the miR-19b-3p /LINC00667/CTGF signaling pathway.

2. Materials and methods

2.1. Study subjects

A total of 138 patients diagnosed with CRF from Linyi People's Hospital were recruited for the purposes of our study. There were 81 males and 57 females aged between 22 and 53 years (mean age of 40.03 ± 5.69 years). The course of disease among the patients ranged from 11 months to 5 years, with a mean course of 1.58 years. Patients from Linyi People's Hospital free of CRF served as the control group as depicted in Table 1. The status of all patients was confirmed by means of clinical diagnosis as well as a series of examinations. The diagnostic criteria employed were complied with the CKD staging criteria of the K/DOQI guidelines, as illustrated in Table 2. The primary diseases detected included 38 cases of diabetic nephropathy (the course of disease ranged from 7 tears to 17 years with a mean course of 9.5 ± 6.8 years), 44 cases of chronic glomerulonephritis, 29 cases of benign arteriolar sclerosis, 14 cases of polycystic kidney, 8 cases of lupus kidney, and 5 cases of gouty kidney. Prior to enrollment to the study, all patients signed informed consents. The experiment was approved by the clinical laboratory ethics committee at Linyi People's Hospital.

2.2. Immunohistochemistry

Normal renal tissues from CRF free men and women aged 35–50 years were obtained at Linyi People's Hospital. Both the normal and CRF tissues were fixed with 10% formaldehyde and dewaxed in xylene twice (10 min each time), dehydrated in gradient ethanol (100%, 95%, 75% and 50%, 5 min each time), washed with distilled water for 5 min, washed in phosphate buffer saline (PBS) for 5 min, followed by the addition of 1 drop of H_2O_2. The tissues were then incubated for 10 min at room temperature, washed with PBS 3 times (3 min each time), added with citric acid (pH = 6.0), repaired in a microwave for 20 min, and then washed 3 times with PBS (3 min each time). The tissues were cultured for 5 min at room temperature after the addition of one drop of normal goat serum. After the serum was removed, the tissues were incubated with rabbit polyclonal CTGF antibody (1: 200, ab5079, Abcam Inc., Cambridge, MA, USA) overnight either at 4 °C or at 37 °C for 1 h. After 3 PBS washes (3 min each time), the tissues were incubated with biotinylated goat anti-rabbit secondary antibody (SE134, Beijing Solarbio Science & Technology Co., Ltd., Beijing, China) at 37 °C for 30 min. After an additional 3 PBS washes (3 min each time), the tissues were developed using daminobenzidine (DAB, Wuhan Boster Biological Technology Ltd., Wuhan, Hubei, China) for 1–2 min followed by three additional PBS washes (2 min each time). The tissues were then counter-stained with hematoxylin (Nanjing Kaiji Biological Engineering Co., Ltd., Nanjing, Jiangsu, China) for 1 min, dehydrated, cleared and sealed with neutral gum. The known positive sections were employed as the positive control, while PBS was regarded as the negative control (NC) in place of the primary antibody. Five representative high-power fields were observed under a positive light microscope (NIKON, Tokyo, Japan) and counted. The positive result was identified as brown and yellow cytoplasm. The tissues were made into paraffin blocks, cut into 3-μm serial sections and performed with MASSON staining. With 10 non-overlapped fields in cortical area selected in each section and observed, the percentage of positive area of Masson-stained rearenal interstitium on the total fields in each section was calculated using HPLAS-1000 pathological analysis system, and then the semi-quantitative analysis for renal interstitial fibrosis was conducted.

Table 1
Baseline information of patients with CRF and normal controls.

Baseline information	The control group	The CRF group	p
n	42	138	
Gender (male/female)	25/17	81/57	0.924
Age (years)	41.31 ± 6.17	40.03 ± 5.69	0.212
Systolic pressure (mmHg)	121.59 ± 14.26	119.42 ± 13.32	0.364
Diastolic pressure (mmHg)	83.28 ± 7.15	82.13 ± 6.23	0.313
Fasting blood-glucose (mmol/L)	5.92 ± 0.52	6.01 ± 0.48	0.298
TC (mmol/L)	4.23 ± 0.65	4.28 ± 0.71	0.684
TG (mmol/L)	1.37 ± 0.31	1.33 ± 0.24	0.380
Smoking [n (%)]	15 (35.71)	49 (35.51)	0.980
Drinking [n (%)]	11 (26.19)	38 (27.54)	0.864
History of hypertension [n (%)]	19 (45.24)	65 (47.10)	0.832
Diabetes mellitus [n (%)]	8 (19.05)	38 (27.53)	0.269
Serum creatinine (μmol/L)	97.42 ± 11.8	340.51 ± 98.6	< 0.0001
BUN (mmol/L)	9.06 ± 2.09	22.95 ± 8.96	< 0.0001
Glomerular filtration rate (mL/min)	63.87 ± 11.07	27.31 ± 1.47	< 0.0001
Proteinuria (g/24 h)	0.87 ± 0.09	2.86 ± 0.48	< 0.0001

Notes: CRF, chronic renal failure; TC, total cholesterol; TG, triglycerides; BUN, blood urea nitrogen.

2.3. Reverse transcription quantitative polymerase chain reaction (RT-qPCR)

The total RNA was extracted using the Trizol RNA (Invitrogen Inc., Carlsbad, CA, USA) extract. The integrity of the extracted RNA was determined by agarose gel electrophoresis means. The bands of 28S and 18S were observed to be bright, clear and sharp, while the brightness of

Table 2
CKD staging criteria of the K/DOQI guidelines.

Stage	AER (mg/24 h)	ACR	PER (mg/24 h)	PCR	Determination of urinary protein	Condition	Cases
A1	< 30	< 30	< 150	< 150	Negative	Normal or mild elevation	33
A2	30–300	30–300	150–500	150–500	+	Moderate elevation[a]	47
A3	> 300	> 300	> 500	> 500	+ or above	Severe elevation[b]	58

Notes: CKD, chronic kidney disease; AER, albumin excretion rate; ACR, albumin creatinine ratio (mg/24 h); PCR, protein creatinine ratio.
[a] Compared with young adult level.
[b] Nephrotic syndrome (AER > 2200 mg/24 h, ACR (mg/mmol) > 220).

the 28S was two times that of 18S band after detection, confirming that the RNA fragment was intact. The ratio of A260 and A280 was determined to be 1.8–2.1 at 260 nm (A260) which was detected using the spectrophotometric method, indicating the high purity of RNA. Reverse transcription was performed using a Primescript TMRTreagent Kit (RR037A, Takara Biotechnology Inc., Dalian, Liaoning China). The reaction conditions applied were as follows: 1 μL RNA precipitation, 2 μL OdT and 3 μL RNA sample were dissolved by RNAase-free water with the concentration of 40 mL/tube. The samples were heated at 70 °C for 5 min and cooled down on ice for 2 min. The samples were then supplemented with 1 μL of dNTP, 1 μL of RNA enzyme inhibitor, 5 μL of 5 × reverse transcription buffer and 1 μL of reverse transcriptase MMLV and bathed at 37 °C for 90 min after being mixed evenly using transfer pipette. The samples were heated for 5 min at 70 °C allowing for termination of the reaction, and then stored on an ice box for later experimentation. A PCR instrument (ABI 7500, Applied Biosystems, Foster City, CA, USA) was utilized to amplify the target genes as well as the internal references. The reaction system included 25 μL of 10 × PCR Buffer, 2.5 μL of 25 mmol/L $Mgcl_2$, 1.5 μL of 10 mmol/L dNTP, 0.5 μL of 10 mmol/L Primer, 1 μL of 1 nmol/L Probe, 0.25 μL of Taq, 2.5 μL of cDNA and 15 μL of sterile distilled water. The reaction conditions consisted of denaturation at 94 °C for 5 min, 94 °C for 30 s, 58 °C for 45 s and 72 °C for 30 s with 40 cycles and extension at 72 °C for 10 min. The reactions were set with three duplicated wells. U6 served as the internal interference for miR-19b-3p, while glyceraldehyde-3-phosphate dehydrogenase (GAPDH) was the internal reference for the other factors. The experiment was repeated three times. The primer sequences are depicted in Table 3.

Table 3
Primer sequences for RT-qPCR.

Genes	Sequences (5′-3′)
miR-19b-3p	F: TGATAATTAGCAAGCAGGATTA
	R: ACCAACATTACGCGGCATCATTA
U6	F: CTCGCTTCGGCAGCACA
	R: AACGCTTCACGAATTTGCGT
LINC00667	F: GTGGGTAGGAAACAGTCGGG
	R: CTCAAAGGTGGCCAAAAGCC
TGF-β1	F: CCCAGCATCTGCAAAGCTC
	R: GTCAATGTACAGCTGCCGCA
CTGF	F: TTGCGAAGCTGACCTGGAA
	R: TGCTGGTGCAGCCAGAAA
α-SMA	F: CACTGCCTTGGTGTGTGACAAT
	R: CGTAGCTGTCTTTTTGTCCCATTC
TIMP-1	F: TTCGTGGGGACACCAGAAGTCAAC
	R: TGGACACTGTGCAGGCTTCAGTTC
GAPDH	F: TTCCAGGAGCGAGATCCCT
	R: CACCCATGACGAACATGGG

Notes: RT-qPCR, reverse transcription quantitative polymerase chain reaction; F, forward; R, reverse; TGF-β1, transforming growth factor β1; CTGF, connective tissue growth factor; α-SMA, alpha smooth muscle actin; TIMP-1, tissue inhibitor of metalloproteinase-1; GAPDH, glyceraldehyde-3-phosphate dehydrogenase.

2.4. Western blot analysis

Lysate (C0481, Sigma-Aldrich Chemical Company, St Louis, MO, USA) was used to extract the total proteins while the bicinchoninic acid (BCA) protein method was applied for protein quantification purposes. Next, 10% sodium dodecyl sulfate-polyacrylamide gel electrophoresis (SDS-PAGE) gel was prepared with 20 μg of protein placed in each well. The samples were mixed with sample buffer and boiled for 5 min at 100 °C. Electrophoretic separation was conducted after ice bath and centrifugation. The proteins on gel were then transferred to the nitrocellulose membrane. Membrane blockade was then conducted with 5% skimmed milk for 1 h, and incubated with rabbit anti-human transforming growth factor-beta 1 (TGF-β1, ab92486, 1: 500), rabbit anti-human CTGF (ab5097, 1: 1000), rabbit anti-human α-smooth muscle actin (α-SMA, ab5694, 1: 500) and rabbit anti-human tissue inhibitor of metalloproteinases-1 (TIMP-1, ab211926, 1: 1000), N-cadherin (ab76057, 1: 1000), Vimentin (ab8978, 1: 1000), and E-cadherin (ab76055, 1: 1000) at 4 °C overnight. All the aforementioned antibodies were purchased from Abcam Inc. (Cambridge, MA, USA). On the following day, the membrane was washed three times using Tris-buffered saline with Tween-20 (TBST) (5 min per wash), followed by incubation with horseradish peroxidase (HRP)-labeled goat anti-rabbit immunoglobulin G (IgG, 1: 500, Beijing ComWin Biotech Co., Ltd., Beijing, China) for 1.5 h at room temperature and washed with TBST. SuperSignal®West DuraExtended Duration Substrate was applied, and 1 mL ECL working solution was prepared according to the instructions. The membrane was incubated and transferred for 1 min and sealed with fresh-keeping film after the excess solution was discarded. In the dark box, the membrane was treated in X-ray film for 5–10 min, followed by development. GAPDH was considered as the internal reference. The primary antibody was mouse anti-human GAPDH (1: 500, Beijing ComWin Biotech Co., Ltd., Beijing, China), and secondary antibody was HRP-labeled goat anti-rat IgG (1: 2000, Beijing ComWin Biotech Co., Ltd., Beijing, China). Methods of incubation were the same as the above method. The relative expressions of TGF-β1, CTGF, α-SMA and TIMP-1 were calculated using the ratio of optical density (OD) values of TGF-β1, CTGF, α-SMA and TIMP-1 to the average gray value of the developing image of the GAPDH band. Image J software (Bio-Rad Laboratories, Inc., Hercules, CA, USA) was employed for the gray value analysis of the target bands. The experiment was repeated three times. The method was applicable for the cell experiments.

2.5. Dual luciferase reporter gene assay

The websites at www.herbbol.org [39] and www.targetscan.org [40] were explored in order to analyze the binding sites between miR-19b-3p and CTGF as well as between that of miR-19b-3p and LINC00667, in order to obtain the sequences containing the function site. The full length of 3′ untranslated region (UTR) area of LINC00667 and CTGF amplification genes was cloned. PCR products were cloned into the pmirGLO Dual Luciferase vector (Promega Corporation, Madison, WI, USA) downstream of the luciferase gene through endonuclease site of *Spe*I and Hind III to construct the pLINC00667-wild type (Wt) group and the pCTGF-Wt group. A target gene database was

applied in an attempt to predict the binding sites of miR-19b-3p and its target genes. The pLINC00667-mutant type (Mut) vector and the pCTGF-Wt vector were constructed using PCR-based site-directed mutagenesis method. Renilla luciferase expression vector pRL-TK (Takara Biotechnology Inc., Dalian, Liaoning, China) was employed as the internal reference. The miR-19b-3p mimic as well as NC was subsequently co-transfected into the cells with luciferase reporter vectors, respectively. Based on the dual-luciferase reporter assay system (Promega, Madison, WI, USA), the dual luciferase activity was detected. The experiment was repeated three times.

2.6. Fluorescence In Situ Hybridization (FISH) assay

FISH assay was applied to identify the subcellular localization of RNA LINC00667 in cells according to the instructions of RiboTMlncRNA FISH Probe Mix (Red) (Guangzhou RiboBio Co., Ltd., Guangzhou, China). The specific steps were as follows: the cover glass was placed in 24-well plate, and then the cells were then inoculated at the density of 6×10^4/well until cell confluence reached about 80%. After the cover glass was taken out, cells were washed by PBS and fixed by 1 mL 4% paraformaldehyde at room temperature. Next, after treatment with protease K, glycine and ethyl phthalide reagent, cells were added with 250 μL prehybridization solution and incubated at 42 °C for 1 h. After removal of prehybridization solution, cells were added with 250 μL hybridization solution RNA LINC00667 (300 ng/mL) containing probe and hybridized at 42 °C overnight. Subsequently, cells were washed with phosphate buffer saline-Tween 20 (PBST) 3 times, added with 4′,6-diamidino-2-phenylindole (DAPI) (ab104139, 1: 100, Abcam, Shanghai, China) diluted by PBST to stain nucleus and added into the 24-well plate to stain for 5 min. Lastly, cells were washed with PBST 3 times (3 min each time), mounted by anti-fluorescence quenching agent, observed and photographed under fluorescence microscope (Olympus Optical Co., Ltd., Tokyo, Japan).

2.7. RNA Binding Protein Immunoprecipitation (RIP) Assay

RIP assay was conducted to examine the binding of RNA LINC00667 and miR-19b-3p and the binding of RNA LINC00667 and AGO2 protein using the Magna RIP RNA-Binding Pretein Immunoprecipitation kit (Millipore, Massachusetts, USA). The renal tubular epithelial cell were washed with pre-cooled PBS with supernatant discarded, lysed by the equal amount of RIPA lysate (P0013B, Beyotime Biotechnology Co., Shanghai, China) on ice for 5 min, centrifuged at 35068 ×*g* at 4 °C for 10 min with supernatant collected. The cell extract was incubated with antibody for co-precipitation, and the specific steps were as follows: 50 μL magnetic beads selected from each co-precipitation reaction system were washed, suspended in 100 μL RIP Wash Buffer (EHJ-BVIS08102, Xiamen Jiahui Biotechnology Co., Ltd. Xiamen, China) and incubated with 5 μg antibody for combining. The magnetic bead-antibody compound was then washed, suspended in 900 μL RIP Wash Buffer, added with 100 μL cell extract for incubation at 4 °C overnight. The samples were placed on magnetic base to collect magnetic bead-protein compound. Then, the samples and Input were detached by protease K respectively to extract RNA, which was used for following PCR detection. The antibodies used in RIP assay were as follows: AGO2 (ab32381, 1: 50, Abcam, Cambridge, UK) mixed for 30 min at room temperature and IgG (1: 100, ab109489, Abcam, Cambridge, UK) used as negative control.

2.8. RNA-pull down assay

The renal tubular epithelial cells were transfected by 50 nM biotin-labeled Bio-probe NC, Bio-RNA LINC00667-WT and Bio-RNA LINC00667-MUT for 48 h, then collected and washed by PBS. The cells were incubated in specific lysis buffer (Ambion, Austin, Texas, USA) for 10 min. Lysate was incubated with the M-280 streptavidin magnetic bead (S3762, Sigma-Aldrich Chemical Company, St Louis, MO, USA) pre-coated by RNase-free bovine serum albumin (BSA) and yeast tRNA (TRNABAK-RO, Sigma-Aldrich Chemical Company, St Louis, MO, USA). The magnetic bead was incubated at 4 °C for 3 h, washed by precooled lysate 2 times, by low salt buffer 3 times and by high-salt buffer once. The combined RNA was purified by Trizol and then performed with RT-qPCR to examine the miR-19b-3p enrichment.

2.9. Model establishment and grouping

A total of 67 clean grade Spague-Dawlay (SD) male rats weighing between 200 and 250 g were provided by the Animal Center of Zhong Shan Medical University (Guangzhou, Guangdong). The rats were raised under room temperature conditions of 18–22 °C and were provided with free access to food, water, natural light, at relative humidity of conditions between 40% - 70% and noise of < 50 dB. The CRF models were established after a one-week period of adaptive feeding. The experimental procedure and animal use program have been approved by the animal ethics committee of Linyi People's Hospital.

The rat CRF model was established by removing the right kidney and 2/3 of the left kidney. The rats were intraperitoneally injected with 30 mg/kg of 2% pentobarbital sodium. After being routinely shaved, disinfected and covered with sterilize surgical towels, the rats were fixed on the board in a supine position. An incision was made 1.5 cm left of the inside ventrimeson and 1 cm down, and the right kidney was then exposed followed by ligation of the renal pedicle. After the right kidney had been promptly removed, the abdominal cavity was closed. The muscle and skin were then sutured in a layer by layer fashion, with tetracycline ointment subsequently applied to the wound postoperatively. After the left kidney had been exposed, the fat capsule was stripped and the renal pedicle was clamped using an artery clamp. The upper, lower and lateral portions of the renal 2/3 tissue were resected within a 1 min period. Compression hemostasis was treated using a gelatin sponge, followed by the immediate removal of the arterial clamp. The reset was conducted when surface of remnant kidney displayed no signs of bleeding. Next, the abdominal cavity was closed. The muscle and skin were then sutured in a layer by layer fashion, followed by the application of tetracycline ointment to the wound postoperatively. One week post model establishment, transfection was conducted. Seven rats failed to survive during the model establishment process, while the remaining 60 rats were assigned into the blank group (without any transfection), negative control (NC) group (transfection with control dsRNA), siLINC00667 group (transfection with siLINC00667), miR-19b-3p mimic group (transfection with miR-19b-3p mimic), miR-19b-3p inhibitor group (transfection with miR-19b-3p inhibitor) and miR-19b-3p inhibitor + si-LINC00667 group (co-transfection with siLINC00667 and miR-19b-3p inhibitor). The target plasmids (NC, siLINC00667, miR-19b-3p mimic and miR-19b-3p inhibitor) were all purchased from Dharmacon Inc. (Lafayette, CO, USA). Next, 20 μg of NC, 20 μg of siLINC00667, 20 μg of miR-19b-3p mimic, 20 μg of miR-19b-3p inhibitor, 20 μg of siLINC00667 + miR-19b-3p inhibitor (at a concentration of 5 μg/μL dissolved with RNAase-free water) and 3.2 μL of *in vivo*-jetPEITM (PT-201-10G, Polyplus, lllkirch, France) were added to the 5% glucose solution in order to prepare a 50 μL transfection complex followed by incubation at room temperature for 15 min. The transfection complex was injected into rats *via* the tail vein. At the 4th day post transfection, the following experiment was conducted.

2.10. Hematoxylin and eosin (HE) staining and Masson staining

At the 4th d post transfection, the rats were executed and their respective renal tissues were extracted. The tissues were fixed over a 24 h period with 10% neutral formaldehyde solution, dehydrated with alcohol, cleared with xylene, immersed in wax and embedded with paraffin. The samples were then continuously sectioned (5 μm) and stored in an oven at 80 °C for 1 h. After being cooled, the sections were

conventionally dehydrated with gradient alcohol, cleared in xylene and then washed. Then sections were stained with hematoxylin for 4 min, washed, differentiated with hydrochloric acid alcohol for 10 s, rinsed and soaked for 5 min. After turning blue with ammonia for 10 min, the sections were stained with eosin for 2 min, dehydrated with gradient alcohol and sealed with neutral balsam in ventilator. The pathological changes of the renal tissues were analyzed under an optical microscope. The tissues were made into paraffin blocks, cut into 3-μm serial sections and performed with Masson staining. With 10 non-overlapped fields in cortical area selected in each section and observed, the percentage of positive area of MASSON-stained rearenal interstitium on the total fields in each section was calculated using HPLAS-1000 pathological analysis system, and then the semi-quantitative analysis for renal interstitial fibrosis was conducted.

2.11. Enzyme-linked immunosorbent assay (ELISA)

Blood samples (0.5 mL) were obtained from both patient and rat orbits and placed in a 2 mL tube, allowed to stand at a 4 °C refrigerator for 15 min, centrifuged at 11450 ×*g* for 10 min followed by serum collection. Blood urine nitrogen (BUN) was determined using a urease glutamate dehydrogenase kinetic method, calreticulin (CR) with bitter acid dynamic method, fibronectin (FN) with immunoturbidimetry (Shanghai Biological Products Institute, Shanghai, China), and type-IV collagen (CL-IV) with radioimmunoassay. The kits (20,020,901, 20,030,401, 20,031,001 and 20,040,301) were provided by Biotechnology Center of Shanghai Naval Medical Research Institute (Shanghai, China). The employed ELISA kit was balanced at room temperature for 20 min in order to prepare the washing solution. After being dissolved, 100 μL standard substance was added into the reaction plate to plot standard curves, after which 100 μL the sample was added to the reaction wells and incubated for 90 min at 37 °C. After washing, 100 μL biotinylated antibody working solution was added to the sample and incubated for 60 min at 37 °C. The sample was then supplemented with 100 μL enzyme binding agent working solution under conditions void of light, cultured at 37 °C for 30 min and washed three times. The sample was then added with 100 μL substrate and incubated at 37 °C under conditions void of light for 15 min. The reaction was then terminated after the terminal solution was added. A universal microplate reader (BioTek Synergy 2) was applied in order to detect the OD value in each tube at 450 nm within 3 min, followed by measurement of the contents of BUN, serum creatinine (SCR), creatinine clearance rate (CCR), FN and CL-IV in the supernatant of serum subsequently analyzed.

2.12. Cell counting kit-8 (CCK-8) assay

The renal tubular epithelial cells of each group were separated using the Percoll method and inoculated into a 96-well plate with 100 μL cell culture medium in each well. The cell density was then adjusted to 2×10^3 cells/mL. The cells were cultured in a culture box at 37 °C, with cell viability detected at 24 h, 48 h and 72 h. The samples were then added with 10 μL CCK8 reagent (C0037, Beyotime Biotechnology Co., Shanghai, China) and incubated at 37 °C for 2 h. A microplate reader (Multiskan FC, Thermo Fisher Scientific Inc., Waltham, MA, USA) was applied for detecting and counting purposes. The OD value was confirmed to be 450 nm/630 nm. Each group was set with three parallel wells and the mean value was subsequently calculated. A cell viability curve was constructed with time as the abscissa and the OD value as vertical axis. The experiment was conducted 3 times.

2.13. Scratch test

The renal tubular epithelial cells of each group were separated using the Percoll method. Six groups of 6-well plates were selected, while the cells were then grouped. The lines were drawn on the back of the 6-well plate every 0.5 to 1 cm using a mark pen and crossed the well with 5 lines at least. The 5×10^5 cells were added to each of the 6-well plates and cultured overnight. With a pipette head perpendicular to the line, scratches were created the next day. The cells were then washed three times with PBS and added with serum-free medium after the scratched cells had been removed. The samples were then incubated at 37 °C in an incubator with 5% CO_2. After the samples had been collected at 0 and 24 h, the migration distance was evaluated under an inverted microscope (× 100). The experiment was repeated 3 times.

2.14. Flow cytometry

After 48-h of transfection, the culture medium was removed and the renal tubular epithelial cells were then washed with PBS. The cells were treated with 0.25% trypsin. Cells were found to have shrunk and were round in shape when observed under a microscope following the removal of trypsin. Culture medium containing serum was added to terminate the detachment. The cells were triturated and prepared into a cell suspension which was then centrifuged at 178 ×*g* for 5 min, with the supernatant then removed. The cells were washed twice with PBS, filtered with 60 μm aperture filter and fixed in pre-cooled 70% ethanol for 30 min, centrifuged and collected. After PBS washing, 1% propidium iodide (PI) containing RNA enzyme was added into the cells to stain for 30 min. After that, the cells were washed twice with PBS in order to remove PI, with the cell volume then adjusted to 1 mL with PBS. The cells were subsequently filtered with a 60 μm aperture filter again. The sample was placed into a BD-Aria flow cytometry (FACSCalibur, Beckman Coulter, Brea, CA, USA) in order to detect cell cycle. Three samples were set in each group. The experiment was repeated three times.

After 48-h of transfection, cells were treated with ethylenediaminetetraacetate (EDTA)-free trypsin, collected into a flow tube and centrifuged with the supernatant removed. The cells were then washed three times with cooled PBS and centrifuged with the supernatant discarded. Based on the Annexin V-fluorescein isothiocyanate (FITC)/PI apoptosis detection kit (C1065, Beyotime Biotechnology Co., Ltd., Shanghai, China), Annexin-V-FITC/PI staining solution was prepared at the ratio of 1: 2: 50 of Annexin-V-FITC, PI and N-2-Hydroxyethylpiperazine-N′-2-Ethanesulfonic Acid (HEPES) buffer solution. Next, 100 μL of staining solution was used to suspend 1×10^6 cells followed by the performance of vibration and mixing. The cells were incubated at room temperature for 15 min and added with 1 mL of HEPES buffer, vibrated and mixed in an even manner. FITC and PI fluorescence were evaluated at 525 nm and 620 nm bandpass filters excited by the excitation wavelength of 488 nm to detect cell apoptosis. Three samples were set in each group and the experiment was repeated three times.

2.15. Statistical analysis

The Statistical Package for the Social Sciences (SPSS) version 21.0 (IBM Corp. Armonk, NY, USA) was employed for experimental data statistical analyses. Measurement data were displayed as mean ± standard deviation. The normality of data (Kolmogorov-Smirnov [K-S] method) and the homogeneity of variance (Levene's test) were examined. In the event that the data conformed to the normality of data and the homogeneity of variance, comparisons between two groups were analyzed by independent-sample *t*-test, while comparisons among multiple groups were performed using one-way analysis of variance or repeated-measures analysis of variance with the Tukey's *post hoc* tests for multiple pairwise comparisons. If the data failed to conform to the normality of data or the homogeneity of variance, a rank sum test would be applied. All tests were two-tailed and a *p*-value lower than 0.05 was considered to be statistically significant.

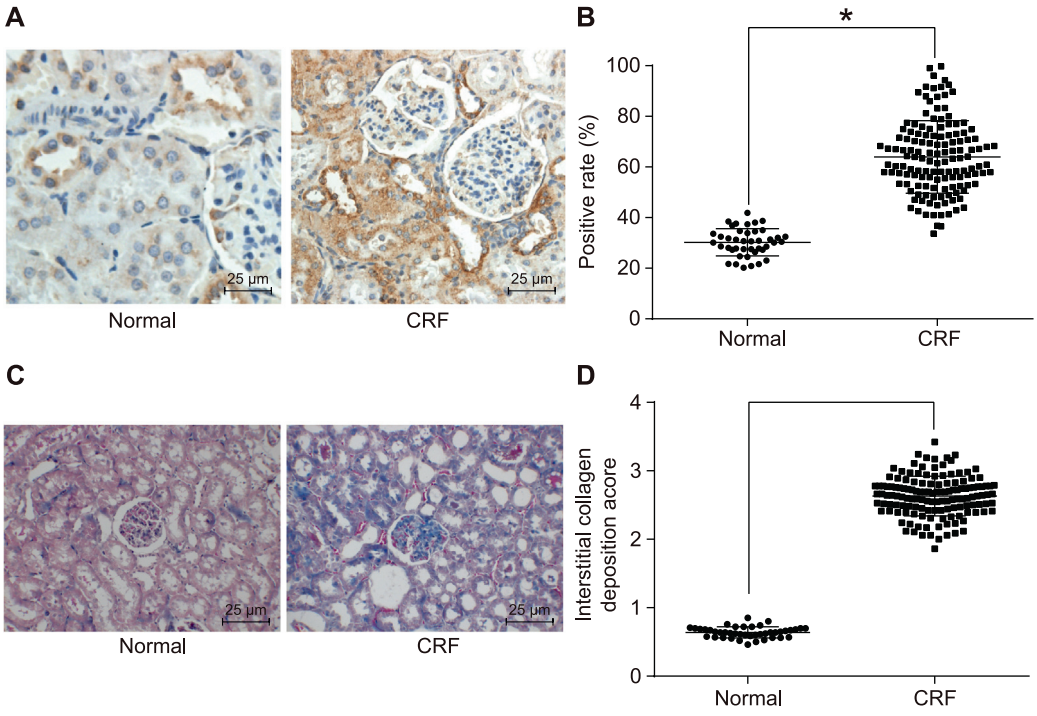

Fig. 1. High positive expression of CTGF is found in CRF tissues (× 400). A, immunohistochemical staining of CTGF in normal renal tissues (n = 42) and CRF tissues (n = 138); B, quantitative analysis of positive expression rate of CTGF in normal renal and CRF tissues; C, fibrosis in normal renal tissues (n = 42) and CRF tissues (n = 138) examined by Masson staining; D, interstitial collagen area in normal tissues and CRF tissues. *, $p < 0.05$ *vs.* the normal renal tissues; measurement data were displayed as mean ± standard deviation; independent sample *t*-test was performed for comparisons between two groups. CTGF, connective tissue growth factor; CRF, chronic renal failure.

3. Results

3.1. Positive expression rate of CTGF is higher in human CRF tissues

Immunohistochemistry methods were employed to detect the positive rate of CTGF, with yellow or tan granules indicated positive expression of CTGF. A small amount of CTGF was found to be positively expressed in the cytoplasm of renal tubular epithelial cells and interstitial cells as well as in the cytoplasm of epithelial cells of the medullary collecting duct in normal renal tissues, while a large amount of CTGF positive expression granules were observed in the epithelial cells of the CRF tissues. CTGF expression was detected in the fibroblast cells of the renal interstitium. According to statistical analysis, the positive expression rate of CTGF in CRF tissues was 63.95%, which was markedly higher than that in the normal renal tissues (30.22%) ($p < 0.05$). Besides, Masson staining was conducted to detect the collagen deposition in renal interstitium of normal tissues and CRF tissues. The results showed that compared with the normal tissues, the CRF tissues presented more collagen depositions ($p < 0.05$) (Fig. 1). The above results suggested that CTGF was highly expressed in CRF.

3.2. Serum levels of BUN, SCR, FN and CL-IV are highly expressed while low expression of CCR are detected in human CRF tissue

ELISA was applied in order to determine the serum levels of BUN, SCR, CCR, FN and CL-IV. The results revealed that compared with the normal renal tissues, there were increased serum levels of BUN, SCR, FN and CL-IV, while descended expression levels of CCR were detected in the serum of patients with CRF (all $p < 0.05$) (Table 4).

3.3. miR-19b-3p negatively targetes lncRNA LINC00667 and CTGF

The biological prediction websites www.herbbol.org and www.targetscan.org provided verification that miR-19b-3p negatively targeted LINC00667 as well as the CTGF gene. The specific binding regions between LINC00667 and miR-19b-3p are displayed in Fig. 2A. The specific binding regions between CTGF and miR-19b-3p are displayed in Fig. 2C. The dual luciferase reporter gene assay results are illustrated in Fig. 2B, D. Compared with the control group, the miR-19b-3p mimic group displayed notably reduced luciferase activity among the cells co-transfected with pLINC00667-Wt and pCTGF-Wt ($p < 0.05$), while no significant difference was observed regarding the luciferase activity of cells transfected with the pLINC00667-Mut and pCTGF-Mut plasmid ($p > 0.05$). These findings provided evidence that lncRNA LINC00667 and CTGF were indeed the direct target genes of miR-19b-3p.

The results of RNA-FISH assay revealed that LINC00667 mainly expressed in cytoplasm (Fig. 2E). The results of RIP assay (Fig. 2F) showed that LINC00667 could bind to AGO2 protein and could target miR-19b-3p. The results of RNA-pull down assay (Fig. 2G) showed that compared with the Bio-probe NC group, the significantly increased miR-19b-3p enrichment was found in the Bio-LINC00667-WT group ($p < 0.05$) while the Bio-LINC00667-MUT group showed no significant difference ($p > 0.05$). The results above suggested that LINC00667 could competitively bind to miR-19b-3p and regulate the homeostasis of miR-19b-3p.

Table 4
Serum levels of BUN, SCR, CCR, FN and CL-IV in patients with CRF.

Groups	Normal (n = 42)	CRF (n = 138)	p
BUN (mmol/L)	11.21 ± 3.24	23.80 ± 4.61*	< 0.001
SCR (μmol/L)	28.83 ± 4.33	73.50 ± 8.84*	< 0.001
CCR (mL/min.m^2)	2.08 ± 0.45	0.74 ± 0.31*	< 0.001
FN (ng/L)	73.25 ± 8.31	149.49 ± 9.12*	< 0.001
CL-IV(μg/L)	12.46 ± 3.37	25.22 ± 5.34*	< 0.001

Notes: CRF, chronic renal failure; BUN, blood urine nitrogen; SCR, serum creatinine; CCR, creatinine clearance rate; FN, fibronectin; CL-IV, type-IV collagen.

* $p < 0.05$ *vs.* the normal renal tissues; the measurement data were expressed as mean ± standard deviation; comparisons between two groups were analyzed by *t*-test.

3.4. miR-19b-3p is down-regulated and LINC00667 is up-regulated in human CRF tissues

RT-qPCR (Fig. 3A) and Western blot analysis (Fig. 3B, C) methods were adopted to detect the expression of lncRNA LINC00667 and miR-

A

Target Name	LINC00667
Target Transcripts	LINC00667-003 LINC00667-001
ClipSeq peakCluster	HPCB1 18401(AGO2 PSR-CLIP BC-1) HPCB3 10078(AGO2 PAR-CLIP BC-3) HHFCT 71660(AGO2 HITS-CLIP Hela) HHFKP 67182(AGO2 HITS-CLIP Hela) HPSEF 10517(AGO2 PAR-CLIP EF3D-AGO2) HPKTA 28579(AGO2 PAR-CLIP HEK293) HPCB1 18402(AGO2 PAR-CLIP BC-1) HPSD3 4661(AGO2 PAR-CLIP LCL-BACD3) HPCB3 10079(AGO2 PAR-CLIP BC-3) HPSD1 4492(AGO2 PAR-CLIP LCL-BACD1)
ClipSeq ReadNum	270
miRNA-target	miRNA 3'-agTCA-AAACGTACCT---AAACGTGt-5' ncRNA 5'-acAGTATTTGCATATAACCTTTGCACa-3'
alignScore	0

B

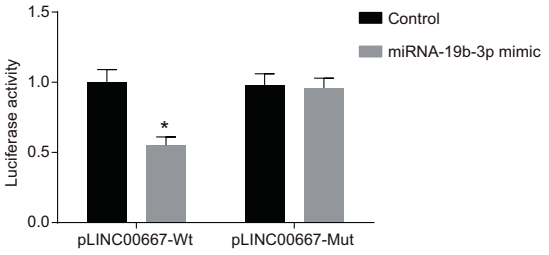

C

	Predicted consequential pairing of target region (top) and miRNA (bottom)
Position 1043-1049 of GTGF 3'UTR hsa-miR-19b-3p	5' ···ACCAAAAGUUACAUG--UUUGCACC··· 3' AGUCAAAACGUACCUAAACGUGG

D

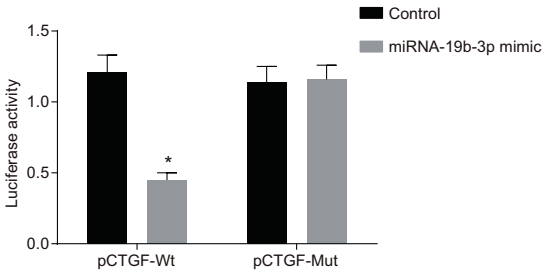

E

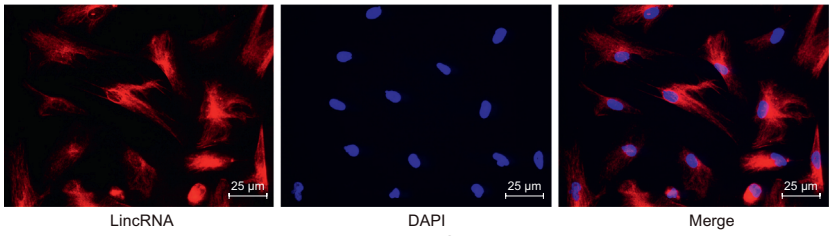

F

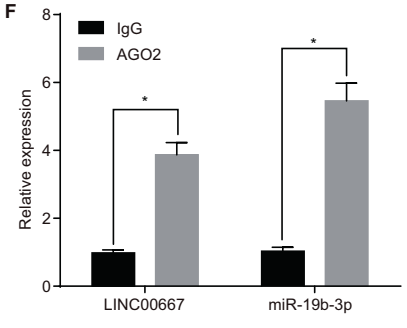

G

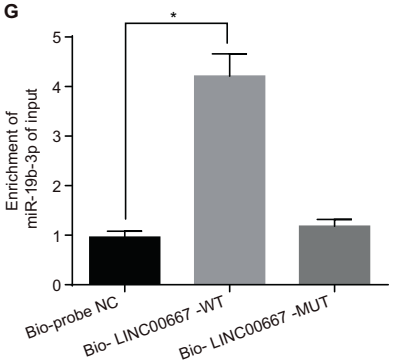

Fig. 2. LINC00667 and CTGF bind to miR-19b-3p. A, binding regions between LINC00667 3'UTR and miR-19b-3p sequence; B, luciferase activity of the pLINC00667-Wt and pLINC00667-Mut after transfection; C, binding regions between CTGF 3'UTR and miR-19b-3p sequence; D, luciferase activity of the pCTGF-Wt and pCTGF-Mut after transfection; E, FISH assay showed that LINC00667 mainly expressed in cytoplasm; F, RIP assay showed that LINC00667 could bind to AGO2 protein and miR-19b-3p, $^{\#}$, $p < 0.05$ *vs.* the IgG group; G, the relationship between LINC006676 and miR-19b-3p examined by RNA-pull down assay, $^{\#}$, $p < 0.05$ *vs.* the Bio-probe NC group; *, $p < 0.05$ *vs.* the control, IgG, or Bio-probe NC groups; measurement data were displayed as mean ± standard deviation; multiple groups were compared by one-way analysis of variance; the experiment was repeated 3 times; CTGF, connective tissue growth factor; miR-19b-3p, microRNA-19b-3p; 3'UTR, 3′ untranslated region; Wt, wild-type; Mut, mutant; FISH, Fluorescence *In Situ* Hybridization; RIP, RNA Binding Protein Immunoprecipitatio; NC, negative control.

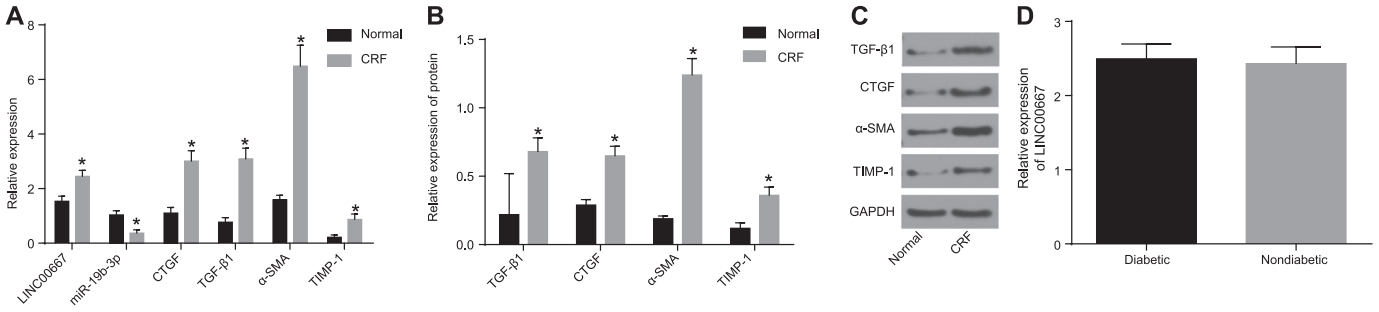

Fig. 3. LINC00667 and CTGF are upregulated while miR-19b-3p is downregulated in patients with CRF. A, LINC00667 and miR-19b-3p expression and mRNA levels of TGF-β1, CTGF, α-SMA and TIMP-1, with GAPDH used as internal reference; B, protein levels of TGF-β1, CTGF, α-SMA and TIMP-1, with GAPDH used as internal reference; C, the gray value of TGF-β1, CTGF, α-SMA and TIMP-1 protein bands with GAPDH as the internal reference; D, the LINC00667 expression between nondiabetic patients and diabetic patients; *, $p < 0.05$ *vs.* the normal renal tissues; independent sample *t*-test was performed for comparisons between two groups; measurement data were displayed as mean ± standard deviation; CRF, chronic renal failure; TGF-β1, transforming growth factor β1; CTGF, connective tissue growth factor; α-SMA, alpha smooth muscle actin; TIMP-1, tissue inhibitor of metalloproteinase-1; GAPDH, glyceraldehyde-3-phosphate dehydrogenase.

19b-3p as well as the mRNA and protein expression of TGF-β1, CTGF, α-SMA and TIMP-1 in the normal renal and CRF tissues. Compared with the normal renal tissues, CRF tissues exhibited distinctly reduced miR-19b-3p expression, while increased lncRNA LINC00667 expression and mRNA and protein expression of TGF-β1, CTGF, α-SMA and TIMP-1 (all $p < 0.05$). Additionally, the comparison of LINC00667 expression between nondiabetic patients and diabetic patients showed no significant difference ($p > 0.05$) (Fig. 3). These findings suggested that miR-19b-3p decreased and lncRNA LINC00667 increased among patients with CRF.

3.5. Overexpressed miR-19b-3p lessens the degree of renal damage

Pathological changes of rat renal tissues were analyzed using HE staining. Distal tubular ectasia, mild vacuolar degeneration in epithelial cells, mild edema in renal interstitium with scattered lymphocytes and macrophage infiltration were observed in the blank, NC and miR-19b-3p inhibitor + siLINC00667 groups while the interstitial collagen area showed no significant difference ($p > 0.05$). Compared with the blank and NC groups, the miR-19b-3p mimic and siLINC00667 groups exhibited improved interstitial edema and inflammatory cell infiltration and significant reduced interstitial collagen area ($p < 0.05$). A key observation was made indicating that in the miR-19b-3p inhibitor group, the renal tubular structure was severely damaged; with signs of atrophy and necrosis of the renal tubules accompanied by dilatation of some tubules; there was evidence of protein cast in some of the lumens, with the collecting duct dilated and collapsed lumen with massive necrosis detected in the epithelial cells and increased interstitial collagen area (Fig. 4). Based on the results obtained it was concluded that miR-19b-3p overexpression could alleviate the degree of renal damage.

3.6. Overexpressed miR-19b-3p decreases serum levels of BUN, SCR, FN and CL-IV while increasing serum CCR level in the CRF rat model

ELISA was employed to determine serum levels of BUN, SCR, CCR, FN and CL-IV. As illustrated in Table 5, no significant difference was observed in relation to the serum levels of BUN, SCR, CCR, FN and CL-IV between the blank and NC groups (all $p > 0.05$). The serum levels of BUN, SCR, FN and CL-IV were reduced, while CCR was increased in both the miR-19b-3p mimic and si-LINC00667 groups compared with the blank and NC groups (all $p < 0.05$); However, increased serum levels of BUN, SCR, FN and CL-IV and decreased CCR was detected in the miR-19b-3p inhibitor group (all $p < 0.05$). The reductions in the expressions of BUN, SCR, FN, CL-IV and increased CCR expressions were observed in the miR-19b-3p inhibitor + si-LINC00667 group were found compared with the miR-19b-3p inhibitor group (all $p < 0.05$). The data obtained suggested that miR-19b-3p overexpression decreased serum levels of BUN, SCR, FN and CL-IV, while elevated CCR in CRF rats.

3.7. Overexpressed miR-19b-3p decreases lncRNA LINC00667 expression and mRNA expressions of TGF-β1, CTGF, α-SMA and TIMP-1

RT-qPCR was employed to detect the expression of lncRNA LINC00667 and miR-19b-3p as well as the mRNA expression of TGF-β1, CTGF, α-SMA and TIMP-1 in the rat tissues. As depicted in Fig. 5, no

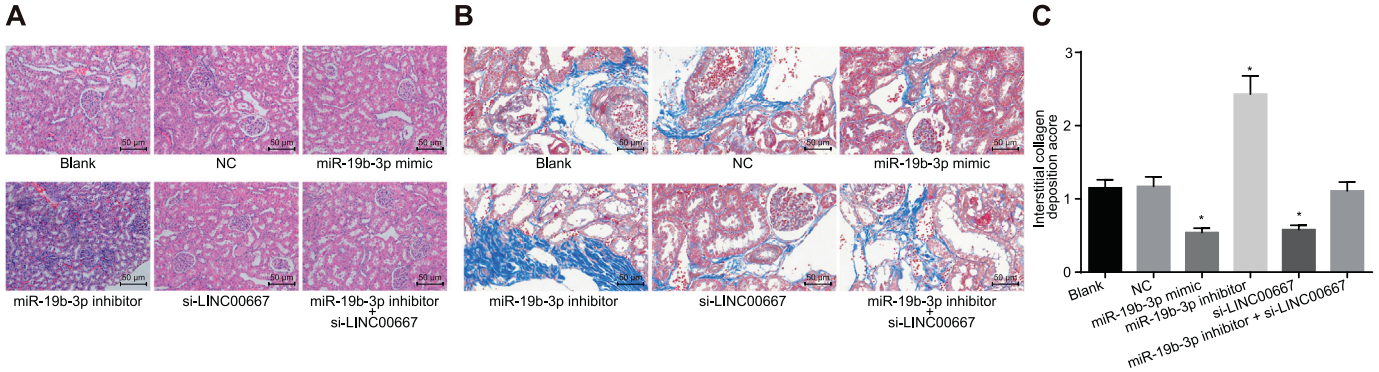

Fig. 4. MiR-19b-3p overexpression alleviates the degree of renal damage in rat models with CRF. A, the renal tissues in each group examined by HE staining (200 ×); B, the renal tissues in each group examined by Masson staining (200 ×); C, the interstitial collagen area of renal tissues in each group, $n = 10$; *, $p < 0.05$ *vs.* the blank and NC groups; measurement data were displayed as mean ± standard deviation and comparisons among multiple groups were analyzed by one-way analysis of variance; the experiment was repeated 3 times. HE, hematoxylin eosin; miR-19b-3p, microRNA-19b-3p; CRF, chronic renal failure; NC, negative control.

Table 5
Serum levels of BUN, SCR, CCR, FN and CL-IV in each group after transfection.

Groups	BUN	SCR	CCR	FN	CL-IV
	(nmol/L)	(μmol/L)	(mL/min.m^2)	(μg/L)	(μg/L)
Blank	13.26 ± 2.10	30.13 ± 1.75	63.56 ± 5.84	168.33 ± 6.75	15.75 ± 1.07
NC	12.65 ± 2.36	28.64 ± 1.53	63.58 ± 5.75	164.56 ± 8.02	15.12 ± 1.01
miR-19b-3p mimic	5.11 ± 1.75*	14.21 ± 1.63*	98.76 ± 8.16*	114.24 ± 7.52*	8.02 ± 1.10*
miR-19b-3p inhibitor	20.12 ± 2.75*	60.23 ± 2.45*	32.41 ± 4.74*	192.5 ± 9.85*	28.42 ± 2.12*
si-LINC00667	5.12 ± 1.72*	13.53 ± 1.23*	99.74 ± 9.15*	115.02 ± 6.57*	8.17 ± 1.02*
miR-19b-3p inhibitor + si-LINC00667	13.64 ± 2.30**	29.85 ± 1.23**	61.57 ± 5.14**	166.52 ± 9.02**	15.02 ± 1.54**

Notes: BUN, blood urine nitrogen; SCR, serum creatinine; CCR, creatinine clearance rate; FN, fibronectin; CL-IV, type-IV collagen.
* $p < .05$ *vs.* the blank and NC groups.
** $p < 0.05$ *vs.* the miR-19b-3p inhibitor group; n = 10; the measurement data were expressed as mean ± standard errors; multiple groups were compared by one-way analysis of variance; the experiment was repeated three times; NC, negative control.

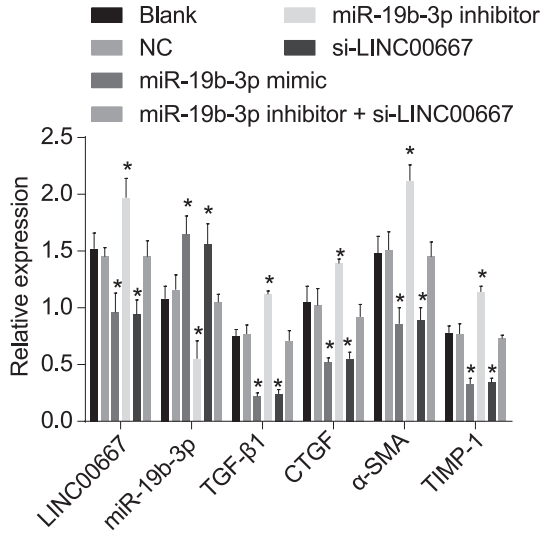

Fig. 5. miR-19b-3p upregulation suppresses LINC00667 expression, mRNA levels of TGF-β1, CTGF, α-SMA and TIMP-1 in rats with CRF. n = 10; *, $p < 0.05$ *vs.* the blank and NC groups; measurement data were displayed as mean ± standard deviation; multiple groups were compared by one-way analysis of variance; the experiment was repeated 3 times; TGF-β1, transforming growth factor β1; CTGF, connective tissue growth factor; α-SMA, alpha smooth muscle actin; TIMP-1, tissue inhibitor of metalloproteinase-1; NC, negative control; miR-19b-3p, microRNA-19b-3p; CRF, chronic renal failure.

notable differences were detected in relation to the expression of lncRNA LINC00667 and miR-19b-3p, and the mRNA expression of TGF-β1, CTGF, α-SMA and TIMP-1 between the blank and NC groups (all $p > 0.05$). Compared with the blank and NC groups, the miR-19b-3p mimic and si-LINC00667 groups exhibited markedly elevated miR-19b-3p expression while significantly decreased mRNA expression of lncRNA LINC00667, TGF-β1, CTGF, α-SMA and TIMP-1 (all $p < 0.05$). However, contrasting results were observed in the miR-19b-3p inhibitor group (all $p < 0.05$). Furthermore, no significant differences in relation to the expression previously mentioned were found in miR-19b-3p inhibitor + si-LINC00667 group (all $p > 0.05$). Therefore, we subsequently concluded that miR-19b-3p overexpression could decrease both lncRNA LINC00667 expression as well as the mRNA expression of TGF-β1, CTGF, α-SMA and TIMP-1.

3.8. Overexpressed miR-19b-3p decreases protein expressions of TGF-β1, CTGF, α-SMA and TIMP-1

Western blot analysis was performed to measure the protein expression of TGF-β1, CTGF, α-SMA and TIMP-1 in the rat tissues. As shown in Fig. 6A, B, there was no significant difference observed in relation to the protein expression of TGF-β1, CTGF, α-SMA and TIMP-1 between the blank and NC groups (all $p > 0.05$). In comparison to the blank and NC groups, the miR-19b-3p mimic and siLINC00667 groups displayed reduced protein expressions of TGF-β1, CTGF, α-SMA and TIMP-1 (all $p < 0.05$), while the miR-19b-3p inhibitor group demonstrated increased protein expressions of TGF-β1, CTGF, α-SMA and TIMP-1 (all $p < 0.05$). Based on the results obtained we concluded that miR-19b-3p overexpression might decrease the protein expressions of TGF-β1, CTGF, α-SMA and TIMP-1.

3.9. Overexpressed miR-19b-3p suppresses EMT in rat models with CRF

Western blot analysis was performed in order to assess the protein expression of N-cadherin, Vimentin, and E-cadherin in the rat tissues respectively. As displayed in Fig. 7A, B, there was no significant difference in protein expression of N-cadherin, Vimentin, and E-cadherin between the blank and NC groups (all $p > 0.05$). In comparison to the blank and NC groups, the miR-19b-3p mimic and si-LINC00667 groups exhibited decreased protein expression of N-Cadherin and Vimentin, but increased expression of E-cadherin (all $p < 0.05$), while the miR-19b-3p inhibitor group demonstrated increased protein expressions of N-cadherin and Vimentin, but decreased expression of E-cadherin (all $p < 0.05$). No significant differences in regard to the protein expression of N-cadherin, Vimentin and E-cadherin in the miR-19b-3p inhibitor + si-LINC00667 group were detected (all $p > 0.05$). Thus, it was concluded that overexpressed miR-19b-3p decreased protein expression of N-cadherin and Vimentin, while increased expression of E-cadherin.

3.10. Overexpressed miR-19b-3p elevates renal tubular epithelial cell viability

CCK-8 assay was used to measure cell viability, as shown in Fig. 8A. No significant difference was observed in relation to cell viability at each time point in the blank and NC groups (all $p > 0.05$). Elevated cell viability in the miR-19b-3p mimic and siLINC00667 groups was detected (all $p < 0.05$), while reduced cell viability was determined in the miR-19b-3p inhibitor group when compared with the blank and NC groups (all $p < 0.05$). No significant difference in relation to cell viability in the miR-19b-3p inhibitor + si-LINC00667 group ($p > 0.05$). The area under the curve (AUC) analysis results (Fig. 8B) displayed the same trend. The results obtained demonstrated that miR-19b-3p overexpression could elevate cell viability.

3.11. Overexpressed miR-19b-3p accelerates renal tubular epithelial cell migration

Scratch tests were employed to measure cell migration. No significant differences were observed in the blank group when compared

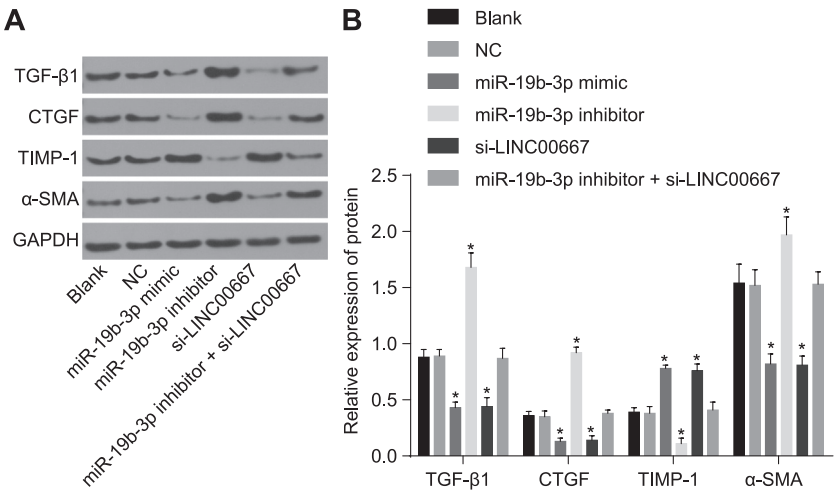

Fig. 6. miR-19b-3p upregulation suppresses protein levels of TGF-β1, CTGF, α-SMA and TIMP-1 in rats with CRF. A, the gray value of TGF-β1, CTGF, α-SMA and TIMP-1 protein bands with GAPDH as the internal reference in response to the treatment of miR-19b-3p mimic, miR-19b-3p inhibitor, si-LINC00667, miR-19b-3p inhibitor + si-LINC00667; B, protein levels of TGF-β1, CTGF, α-SMA and TIMP-1 in response to the treatment of miR-19b-3p mimic, miR-19b-3p inhibitor, si-LINC00667, miR-19b-3p inhibitor + si-LINC00667; n = 10; *, $p < 0.05$ *vs.* the blank and NC groups; measurement data were displayed as mean ± standard deviation; multiple groups were compared by one-way analysis of variance; the experiment was repeated 3 times; TGF-β1, transforming growth factor β1; CTGF, connective tissue growth factor; α-SMA, alpha smooth muscle actin; TIMP-1, tissue inhibitor of metalloproteinase-1; miR-19b-3p, microRNA-19b-3p; CRF, chronic renal failure; GAPDH, glyceraldehyde-3-phosphate dehydrogenase.

with the NC group ($p > 0.05$). Compared with the blank and NC groups, cell migration was significantly increased in the miR-19b-3p mimic and siLINC00667 groups (all $p < 0.05$), while reduced in the miR-19b-3p inhibitor group (all $p < 0.05$). No significant differences in the miR-19b-3p inhibitor + si-LINC00667 group were detected ($p > 0.05$) (Fig. 9A, B). These findings demonstrated that miR-19b-3p overexpression promoted cell migration.

3.12. Overexpressed miR-19b-3p suppresses renal tubular epithelial cell apoptosis

Flow cytometry was performed to detect renal tubular epithelial cell cycle and apoptosis rate, the results of which are displayed in Fig. 10 A-D. No significant differences were detected between the blank and NC groups ($p > 0.05$). Compared with the blank and NC groups, there were less cells arrested at the G_0/G_1 phase, a greater number of cells at the S phase as well as a reduced apoptosis rate in the miR-19b-3p mimic and siLINC00667 groups (all $p < 0.05$). There were fewer cells arrested at the S phase, more at the G_0/G_1 phase, in addition to a higher rate of apoptosis in the miR-19b-3p inhibitor group (all $p < 0.05$). There were no significant differences in the miR-19b-3p inhibitor + si-LINC00667 group (all $p > 0.05$). These findings suggested that miR-19b-3p overexpression could inhibit the renal tubular epithelial cell apoptosis rate as well as resulting in more cells arrested at the S phase.

4. Discussion

CRF remains a major public health stumbling block. Early diagnosis and appropriate management play crucial roles in preventing the progression of CRF to end-stage renal disease (ESRD) [25]. More recently miRNAs that have become a popular research area have been detected in biological fluids including blood and urine, and possess the potential to be disease biomarkers. Moreover, miRNAs have been confirmed to play a role in renal development and disease [26]. Various studies have noted that miRNAs and long non-coding RNAs could modulate renal disease including diabetic nephropathy [27]. Our study provided evidence indicating that repressed LINC00667 and down-regulated CTGF could ameliorate renal fibrosis thus alleviating the CRF.

Initially, we detected there was increased positive expression rate of CTGF, serum levels of BUN, SCR, FN and CL-IV, lncRNA LINC00667 expressions as well as the mRNA and protein expressions of TGF-β1, CTGF, α-SMA, TIMP-1, yet decreased CCR serum level and miR-19b-3p expression in the CRF tissues. CTGF, which is widely thought to contribute to fibrosis, has been suggested to be a possible treatment option with the potential of curing CKD and renal fibrosis [28]. Previous studies have indicated that CTGF can be detected *in vitro* in renal cells with various stimuli, which can lead to fibroblast proliferation, ECM synthesis, and integrin expression. In addition, transforming growth factor-β 1 (TGF-β1) has been reported to promote fibrosis and collagen synthesis in response to renal injury and the serum levels of BUN, SCR and FN

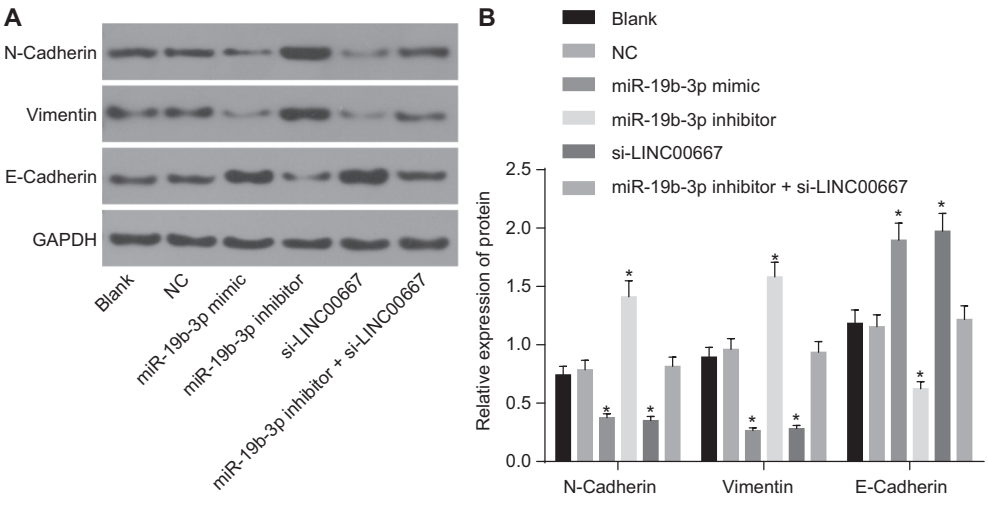

Fig. 7. miR-19b-3p upregulation inhibits EMT in rats with CRF. A, the gray value of N-Cadherin, Vimentin and *E*-Cadherin protein bands with GAPDH as the internal reference in response to the treatment of miR-19b-3p mimic, miR-19b-3p inhibitor, si-LINC00667, miR-19b-3p inhibitor + si-LINC00667; B, protein levels of N-Cadherin, Vimentin and E-Cadherin in response to the treatment of miR-19b-3p mimic, miR-19b-3p inhibitor, si-LINC00667, miR-19b-3p inhibitor + si-LINC00667; n = 10; *, $p < 0.05$ *vs.* the blank and NC groups; measurement data were displayed as mean ± standard deviation; multiple groups were compared by one-way analysis of variance; the experiment was repeated 3 times. EMT, epithelial-mesenchymal transition; miR-19b-3p, microRNA-19b-3p; CRF, chronic renal failure; GAPDH, glyceraldehyde-3-phosphate dehydrogenase.

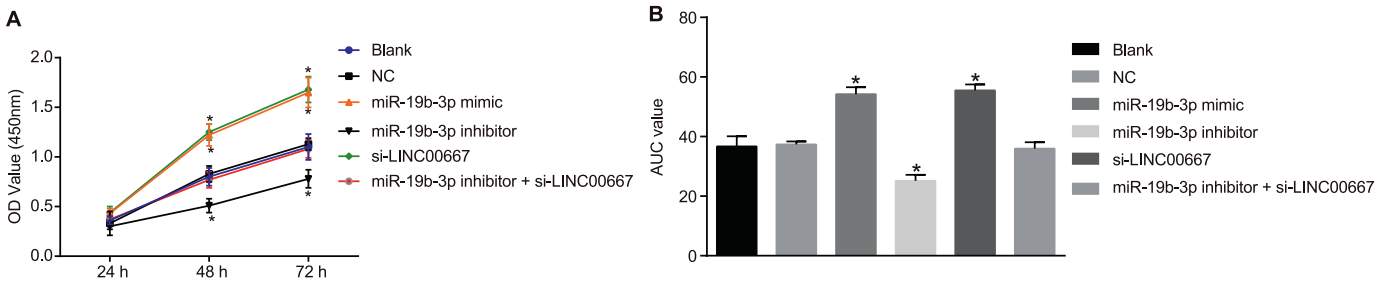

Fig. 8. Overexpressed miR-19b-3p or si-LINC00667 elevates renal tubular epithelial cell viability. A, renal tubular epithelial cell viability detected by CCK-8 assay; B, the AUC value in each group; $n = 3$; *, $p < 0.05$ *vs.* the blank and NC groups; measurement data were displayed as mean ± standard deviation; multiple groups were compared by one-way analysis of variance; the experiment was repeated 3 times. miR-19b-3p, microRNA-19b-3p; AUC, area under the curve; NC, negative control.

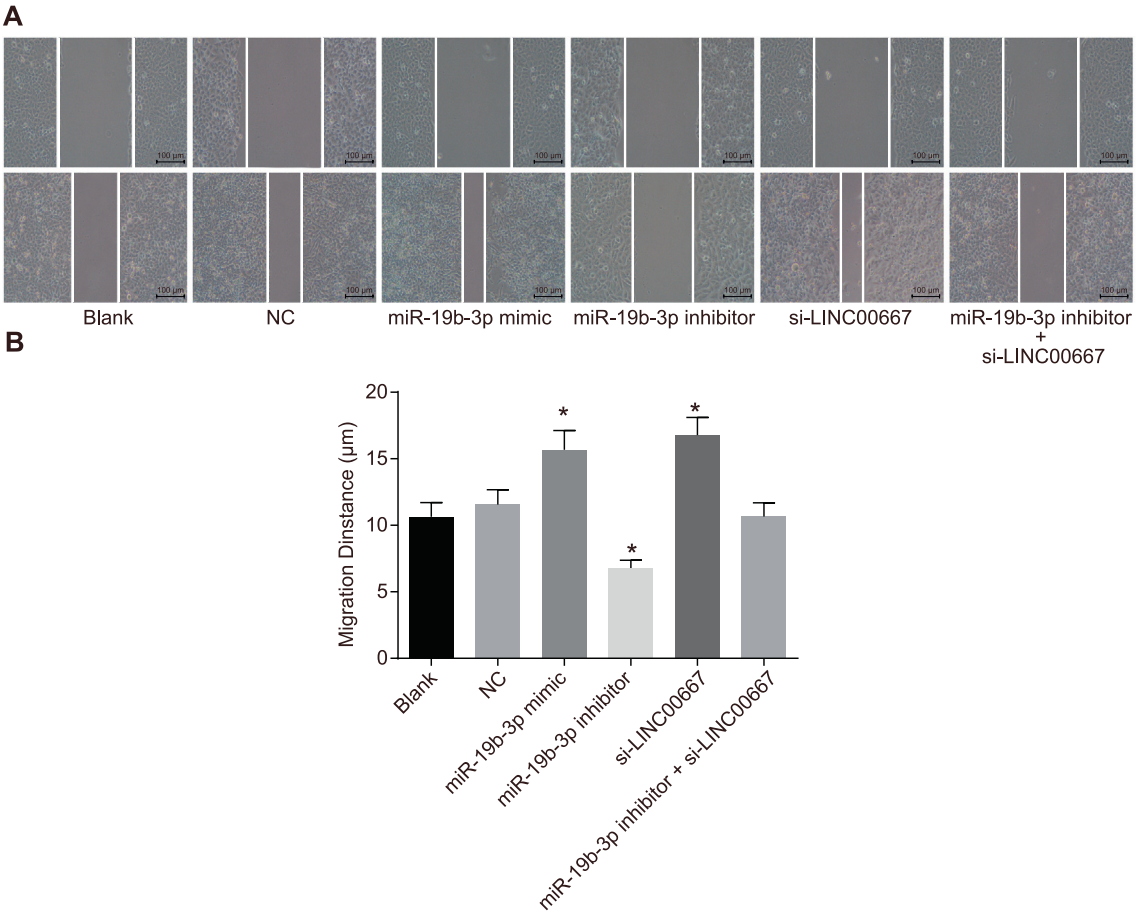

Fig. 9. Overexpressed miR-19b-3p or si-LINC00667 increases renal tubular epithelial cell migration. A, wound-healing condition of renal tubular epithelial cells transfected with miR-19b-3p mimic, miR-19b-3p inhibitor, si-LINC00667, miR-19b-3p inhibitor + si-LINC00667 (× 100); B, migration distance in each group; n = 3; *, $p < 0.05$ *vs.* the blank and NC groups; measurement data were displayed as mean ± standard deviation; multiple groups were compared by one-way analysis of variance; the experiment was repeated 3 times. miR-19b-3p, microRNA-19b-3p; NC, negative control.

were increased in CRF tissues [29,30]. In cases of cystic fibrosis liver disease, elevated TIMP-1, CL-IV and PH have been discovered, all of which have been regarded as indicators of hepatic fibrogenesis in cystic fibrosis [31]. Evidence has been presented supporting the notion that in connection with the down-regulation of α-SMA expression in mesangial cells and renal interstitium, hepatocyte growth factor could help to relieve CRF [32]. CRF is associated with elevated inflammatory markers, which are often observed at the severe stage of CRF and continue to increase with the progression of renal failure [33]. The diagnostic value of CCR based on serum cystatin C (SCys C) has been demonstrated in cases of acute kidney injury [34]. LncRNAs have recently been identified as central regulators in the pathogenesis and progression of cancers, including renal cancer [35]. During the current study, GSE37171 chip suggested that lncRNA LINC00667 was found to be expressed at high levels in CRF tissues. Besides, lncRNA UCA1 has been reported to promote renal cell carcinoma (RCC) proliferation through epigenetically repressing the expression of p21, while negatively regulating miR-495 [35]. Consistently, the knockdown of lncRNA ROR resulted in a decrease of RCC cell proliferation as well as elevated apoptosis *in vitro*, which could also stimulate an increase in the expression of p53 and a decrease in the expression of c-Myc *in vitro* [36]. Interestingly, elevated HOTAIR expression was found in RCC cells when compared with normal renal tissue, and knock-down of HOTAIR reduced migration and decreased proliferation with more cell arrested at

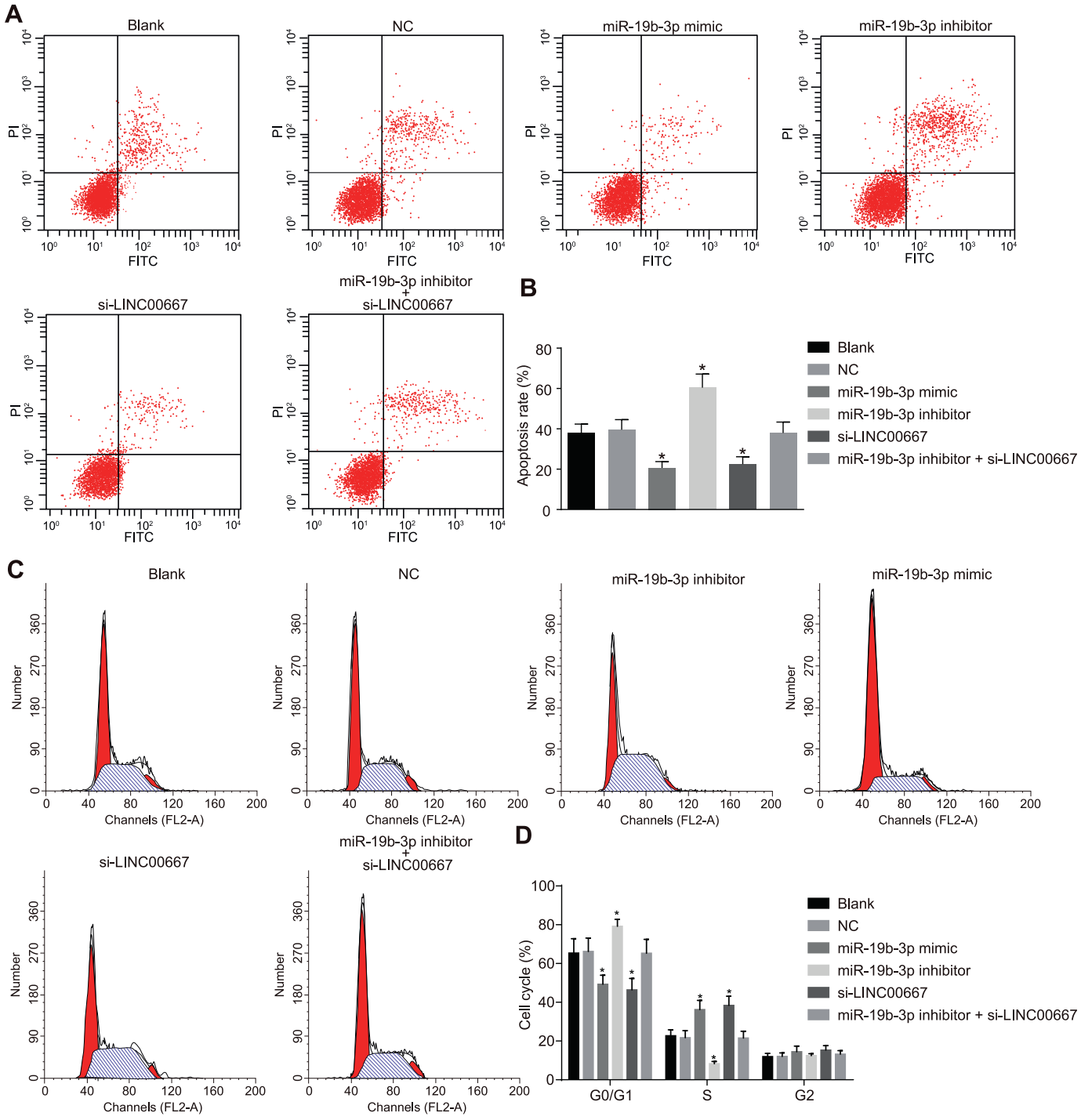

Fig. 10. Flow cytometry shows that overexpressed miR-19b-3p or si-LINC00667 suppresses renal tubular epithelial cell apoptosis. A, flow cytometry map demonstrating renal tubular epithelial cell apoptosis conditions; B, apoptosis rate analysis for renal tubular epithelial cell apoptosis in response to the treatment of miR-19b-3p mimic, miR-19b-3p inhibitor, si-LINC00667, miR-19b-3p inhibitor + si-LINC00667; C, flow cytometry in cell cycle; D, cell cycle in each group; n = 3; *, $p < 0.05$ *vs.* the blank and NC groups; measurement data were displayed as mean ± standard deviation; multiple groups were compared by one-way analysis of variance; the experiment was repeated 3 times. miR-19b-3p, microRNA-19b-3p; CRF, chronic renal failure; NC, negative control.

the G0/G1 phase and less cells at the G2/M phase [37]. In our study, the blockade of lncRNA LINC00667 was determined to play a contributory role in the reduction of the renal tubular epithelial cell apoptosis rate while resulting in an increase of renal tubular epithelial cell migration.

Moreover, we detected decreased lncRNA LINC00667 expression as well as the mRNA and protein expressions of TGF-β1, CTGF, α-SMA and TIMP-1 in rats that were transfected with miR-19b-3p mimic. MiR-19b-3p belongs to both the miR-17-92 and miR-106-363 clusters, which has been shown to play important roles in embryo development, immune system, kidney and heart development, adipose differentiation, aging, and tumorigenicity [18]. The loss of miR-17-92 in nephron progenitors results in a premature depletion of progenitors related to increased apoptosis, leading to the formation of fewer nephrons as well as renal hypodysplasia and striking albuminuria [20]. Studies have revealed that p53 up-regulates CTGF in a human hepatocellular carcinoma cell

line and promotes liver fibrosis by repressing miR-17-92 [38]. The CTGF gene was verified as a target of miR-17-92 in glioblastoma spheroids through the detection of luciferase reporter assays [39], which was in line with our result. miR-17-92 is reported as a potent inhibitor of TGF-β signaling and its activation induces the down-regulation of multiple key effectors along the TGF-β signaling cascade along with direct inhibition of TGF-β-responsive genes [40]. Furthermore, our study also demonstrated that miR-19b-3p might down-regulate lncRNA LINC00667, which (as indicated by www.herbbol.org and www.targetscan.org) has been shown to be a target gene of miR-19b-3p.

In conclusion, the key findings of our study demonstrated that lncRNA LINC00667 could promote fibrosis in CRF through the miR-19b-3p/LINC00667/CTGF signaling pathway, highlighting the therapeutic potential of lncRNAs as well as its promise as a novel prognostic marker.

Competing interests

We declare that we have no conflicts of interest.

Acknowledgments

This study was supported by the Science and Technology Project of Traditional Chinese Medicine in Shandong Province (NO. 2017-467), the Natural Science Project of Shandong Province (NO. ZR2016HP47), Medical and Health Science and Technology Development Plan of Shandong Province in 2018(NO. 2018WSA13029) and the Science and Technology Project of Linyi City (NO. 201616006). We would like to acknowledge the helpful comments on this paper received from our reviewers.

References

[1] A. Ortiz, A. Covic, D. Fliser, D. Fouque, D. Goldsmith, M. Kanbay, F. Mallamaci, Z.A. Massy, P. Rossignol, R. Vanholder, A. Wiecek, C. Zoccali, G.M. London, Board of the, Epidemiology, contributors to, and clinical trials of mortality risk in chronic kidney failure, Lancet 383 (9931) (2014) 1831–1843.
[2] S. Vadakedath, V. Kandi, Dialysis: a Review of the Mechanisms underlying Complications in the Management of Chronic Renal Failure, Cureus. 9 (8) (2017) e1603.
[3] A. Baba, M. Tachi, Y. Ejima, Y. Endo, H. Toyama, K. Saito, N. Abe, M. Yamauchi, C. Miura, I. Kazama, Less contribution of mast cells to the progression of renal fibrosis in Rat kidneys with chronic renal failure, Nephrology (Carlton) 22 (2) (2017) 159–167.
[4] L.G. Fine, J.T. Norman, Chronic hypoxia as a mechanism of progression of chronic kidney diseases: from hypothesis to novel therapeutics, Kidney Int. 74 (7) (2008) 867–872.
[5] B. Rodriguez-Iturbe, G. Garcia Garcia, The role of tubulointerstitial inflammation in the progression of chronic renal failure, Nephron Clin. Pract. 116 (2) (2010) c81–c88.
[6] K.C. Leung, M. Tonelli, M.T. James, Chronic kidney disease following acute kidney injury-risk and outcomes, Nat. Rev. Nephrol. 9 (2) (2013) 77–85.
[7] C.J. Pino, H.D. Humes, Stem cell technology for the treatment of acute and chronic renal failure, Transl. Res. 156 (3) (2010) 161–168.
[8] J.H. Bergmann, D.L. Spector, Long non-coding RNAs: modulators of nuclear structure and function, Curr. Opin. Cell Biol. 26 (2014) 10–18.
[9] B.K. Dey, A.C. Mueller, A. Dutta, Long non-coding RNAs as emerging regulators of differentiation, development, and disease, Transcription. 5 (4) (2014) e944014.
[10] J. Xiong, Y. Liu, L. Jiang, Y. Zeng, W. Tang, High expression of long non-coding RNA lncRNA-ATB is correlated with metastases and promotes cell migration and invasion in renal cell carcinoma, Jpn. J. Clin. Oncol. 46 (4) (2016) 378–384.
[11] X. Zhang, R. Gejman, A. Mahta, Y. Zhong, K.A. Rice, Y. Zhou, P. Cheunsuchon, D.N. Louis, A. Klibanski, Maternally expressed gene 3, an imprinted noncoding RNA gene, is associated with meningioma pathogenesis and progression, Cancer Res. 70 (6) (2010) 2350–2358.
[12] Y. Takahashi, G. Sawada, J. Kurashige, R. Uchi, T. Matsumura, H. Ueo, Y. Takano, H. Eguchi, T. Sudo, K. Sugimachi, H. Yamamoto, Y. Doki, M. Mori, K. Mimori, Amplification of PVT-1 is involved in poor prognosis via apoptosis inhibition in colorectal cancers, Br. J. Cancer 110 (1) (2014) 164–171.
[13] L. Wang, S. Han, G. Jin, X. Zhou, M. Li, X. Ying, L. Wang, H. Wu, Q. Zhu, Linc00963: a novel, long non-coding RNA involved in the transition of prostate cancer from androgen-dependence to androgen-independence, Int. J. Oncol. 44 (6) (2014) 2041–2049.
[14] S. Song, Z. Wu, C. Wang, B. Liu, X. Ye, J. Chen, Q. Yang, H. Ye, B. Xu, L. Wang, RCCRT1 is correlated with prognosis and promotes cell migration and invasion in renal cell carcinoma, Urology 84 (3) (2014) 730 e731–737.
[15] V.K. Topkara, D.L. Mann, Role of microRNAs in cardiac remodeling and heart failure, Cardiovasc. Drugs Ther. 25 (2) (2011) 171–182.
[16] K. Tang, H. Xu, Prognostic value of meta-signature miRNAs in renal cell carcinoma: an integrated miRNA expression profiling analysis, Sci. Rep. 5 (2015) 10272.
[17] T. Huang, L. Yin, J. Wu, J.J. Gu, J.Z. Wu, D. Chen, H.L. Yu, K. Ding, N. Zhang, M.Y. Du, L.X. Qian, Z.W. Lu, X. He, MicroRNA-19b-3p regulates nasopharyngeal carcinoma radiosensitivity by targeting TNFAIP3/NF-kappaB axis, J. Exp. Clin. Cancer Res. 35 (1) (2016) 188.
[18] R. Xie, X. Lin, T. Du, K. Xu, H. Shen, F. Wei, W. Hao, T. Lin, X. Lin, Y. Qin, H. Wang, L. Chen, S. Yang, J. Yang, X. Rong, K. Yao, D. Xiao, J. Jia, Y. Sun, Targeted Disruption of miR-17-92 Impairs Mouse Spermatogenesis by Activating mTOR Signaling Pathway, Medicine (Baltimore) 95 (7) (2016) e2713.
[19] J. Li, S. Yang, W. Yan, J. Yang, Y.J. Qin, X.L. Lin, R.Y. Xie, S.C. Wang, W. Jin, F. Gao, J.W. Shi, W.T. Zhao, J.S. Jia, H.F. Shen, J.R. Ke, B. Liu, Y.Q. Zhao, W.H. Huang, K.T. Yao, D.J. Li, D. Xiao, MicroRNA-19 triggers epithelial-mesenchymal transition of lung cancer cells accompanied by growth inhibition, Lab. Investig. 95 (9) (2015) 1056–1070.
[20] A.K. Marrone, D.B. Stolz, S.I. Bastacky, D. Kostka, A.J. Bodnar, J. Ho, MicroRNA-17~92 is required for nephrogenesis and renal function, J. Am. Soc. Nephrol. 25 (7) (2014) 1440–1452.
[21] H.M. Kok, L.L. Falke, R. Goldschmeding, T.Q. Nguyen, Targeting CTGF, EGF and PDGF pathways to prevent progression of kidney disease, Nat. Rev. Nephrol. 10 (12) (2014) 700–711.
[22] J.R. Montford, S.B. Furgeson, A new CTGF target in renal fibrosis, Kidney Int. 92 (4) (2017) 784–786.
[23] E. Sanchez-Lopez, S. Rayego, R. Rodrigues-Diez, J.S. Rodriguez, R. Rodrigues-Diez, J. Rodriguez-Vita, G. Carvajal, L.S. Aroeira, R. Selgas, S.A. Mezzano, A. Ortiz, J. Egido, M. Ruiz-Ortega, CTGF promotes inflammatory cell infiltration of the renal interstitium by activating NF-kappaB, J. Am. Soc. Nephrol. 20 (7) (2009) 1513–1526.
[24] G.C. van Almen, W. Verhesen, R.E. van Leeuwen, M. van de Vrie, C. Eurlings, M.W. Schellings, M. Swinnen, J.P. Cleutjens, M.A. van Zandvoort, S. Heymans, B. Schroen, MicroRNA-18 and microRNA-19 regulate CTGF and TSP-1 expression in age-related heart failure, Aging Cell 10 (5) (2011) 769–779.
[25] R. Afshar, S. Sanavi, J. Salimi, Epidemiology of chronic renal failure in Iran: a four year single- center experience, Saudi J. Kidney Dis. Transpl. 18 (2) (2007) 191–194.
[26] C.S. Neal, M.Z. Michael, L.K. Pimlott, T.Y. Yong, J.Y. Li, J.M. Gleadle, Circulating microRNA expression is reduced in chronic kidney disease, Nephrol. Dial. Transplant. 26 (11) (2011) 3794–3802.
[27] M.L. Alvarez, M. Khosroheidari, E. Eddy, J. Kiefer, Role of microRNA 1207-5P and its host gene, the long non-coding RNA Pvt1, as mediators of extracellular matrix accumulation in the kidney: implications for diabetic nephropathy, PLoS One 8 (10) (2013) e77468.
[28] P. Boor, J. Floege, Chronic kidney disease growth factors in renal fibrosis, Clin. Exp. Pharmacol. Physiol. 38 (7) (2011) 441–450.
[29] A. Scherer, O.P. Gunther, R.F. Balshaw, Z. Hollander, J. Wilson, R. McManus, W.R. Ng, B.M. McMaster, P.A. Keown McManus, Alteration of human blood cell transcriptome in uremia, BMC Med. Genet. 6 (2013) 23.
[30] J.R. Lu, H.Y. Han, J. Chen, C.X. Xiong, X.H. Wang, J. Hu, X.F. Chen, L. Ma, Protective Effects of Bu-Shen-Huo-Xue Formula against 5/6 Nephrectomy-Induced Chronic Renal failure in Rats, Evid. Based Complement. Alternat. Med. 2014 (2014) 589846.
[31] T.N. Pereira, P.J. Lewindon, J.L. Smith, T.L. Murphy, D.J. Lincoln, R.W. Shepherd, G.A. Ramm, Serum markers of hepatic fibrogenesis in cystic fibrosis liver disease, J. Hepatol. 41 (4) (2004) 576–583.
[32] H.Y. Wang, L.Z. Yang, M.J. Cui, C.M. Gu, Y. Zhao, Y. Chen, D. Zhao, T.S. Li, B. Chi, Hepatocyte growth factor-induced amelioration in chronic renal failure is associated with reduced expression of alpha-smooth muscle actin, Ren. Fail. 34 (7) (2012) 862–870.
[33] H.F. Tbahriti, D. Meknassi, R. Moussaoui, A. Messaoudi, L. Zemour, A. Kaddous, M. Bouchenak, K. Mekki, Inflammatory status in chronic renal failure: the role of homocysteinemia and pro-inflammatory cytokines, World J. Nephrol. 2 (2) (2013) 31–37.
[34] J.T. Hu, X.L. Xie, Z.H. Tang, C.Q. Li, H.W. Zhou, Value of creatinine clearance rate estimated based on serum cystatin C in patients with acute kidney injury, Zhongguo Wei Zhong Bing Ji Jiu Yi Xue. 24 (9) (2012) 534–537.
[35] Y. Lu, W.G. Liu, J.H. Lu, Z.J. Liu, H.B. Li, G.J. Liu, H.Y. She, G.Y. Li, X.H. Shi, LncRNA UCA1 promotes renal cell carcinoma proliferation through epigenetically repressing p21 expression and negatively regulating miR-495, Tumour Biol. 39 (5) (2017).
[36] J. Shi, W. Zhang, H. Tian, Q. Zhang, T. Men, lncRNA ROR promotes the proliferation of renal cancer and is negatively associated with favorable prognosis, Mol. Med. Rep. 16 (6) (2017) 9561–9566.
[37] M. Seles, G.C. Hutterer, T. Kiesslich, K. Pummer, I. Berindan-Neagoe, S. Perakis, D. Schwarzenbacher, M. Stotz, A. Gerger, M. Pichler, Current Insights into Long Non-Coding RNAs in Renal Cell Carcinoma, Int. J. Mol. Sci. 17 (4) (2016) 573.
[38] T. Kodama, T. Takehara, H. Hikita, S. Shimizu, M. Shigekawa, H. Tsunematsu, W. Li, T. Miyagi, A. Hosui, T. Tatsumi, H. Ishida, T. Kanto, N. Hiramatsu, S. Kubota, M. Takigawa, Y. Tomimaru, A. Tomokuni, H. Nagano, Y. Doki, M. Mori, N. Hayashi, Increases in p53 expression induce CTGF synthesis by mouse and human hepatocytes and result in liver fibrosis in mice, J. Clin. Invest. 121 (8) (2011) 3343–3356.
[39] A. Ernst, B. Campos, J. Meier, F. Devens, F. Liesenberg, M. Wolter, G. Reifenberger, C. Herold-Mende, P. Lichter, B. Radlwimmer, De-repression of CTGF via the miR-17-92 cluster upon differentiation of human glioblastoma spheroid cultures, Oncogene 29 (23) (2010) 3411–3422.
[40] P. Mestdagh, A.K. Bostrom, F. Impens, E. Fredlund, G. Van Peer, P. De Antonellis, K. von Stedingk, B. Ghesquiere, S. Schulte, M. Dews, A. Thomas-Tikhonenko, J.H. Schulte, M. Zollo, A. Schramm, K. Gevaert, H. Axelson, F. Speleman, J. Vandesompele, The miR-17-92 microRNA cluster regulates multiple components of the TGF-beta pathway in neuroblastoma, Mol. Cell 40 (5) (2010) 762–773.